Marcin KALINOWSKI, Bogusław BUTRYŁO

Bialystok University of Technology

.doi:10.15199/48.2024.01.43

Dynamic parameters of the ignition coil at various permanent magnet remanence values

Abstract. *The impulse nature of the ignition coils operation imposes specific requirements for the construction of high-voltage windings and magnetoguide. The properties of the system (e.g. pulse energy, inter-turn voltages, operating time) depend on the spatial arrangement of the secondary winding and the materials used. The article considers the properties of the system in which the use of additional magnets with selected remanence was taken into account. The method of modeling the impulse coil, the selection of the operating point with the use of magnets in order to shape the distribution of magnetic field and dynamics of currents and voltages in the system were discussed. The influence of the remanence of magnets on the dynamic characteristics of the current in the primary winding and the voltage in the secondary winding was considered*

Streszczenie. *Impulsowy charakter pracy cewek zapłonowych narzuca specyficzne wymagania dotyczące konstrukcji uzwojeń wysokiego napięcia i magnetowodu. Właściwości układu (m.in. energia impulsu, napięcia międzyzwojowe, czas eksploatacji) zależą od konstrukcji i geometrii uzwojenia wtórnego oraz stosowanych materiałów. W artykule rozpatrzono właściwości układu, w którym uwzględniono zastosowanie dodatkowych magnesów o dobieranej remanencji. Omówiono sposób modelowania cewki impulsowej, dobór punktu pracy z zastosowaniem magnesów w celu kształtowania rozkładu pola oraz dynamiki zmian przebiegów prądów i napięć w układzie. Rozpatrzono wpływ remanencji magnesów na charakterystyki dynamiczne prądu w uzwojeniu pierwotnym i napięcia na uzwojeniu wtórnym. (**Parametry dynamiczne cewki zapłonowej przy różnych wartościach remanencji magnesu trwałego**).*

Keywords: impulse coil, electrodynamics, magnetic field, numerical modelling.
Słowa kluczowe: cewka impulsowa, elektrodynamika, pole magnetyczne, modelowanie numeryczne.

Introduction

The ignition coil is an element responsible for the proper ignition of the air-fuel mixture in the combustion chamber of the internal combustion engine by generating high voltage with appropriate energy on the spark plug electrodes. Commonly used design solutions place more and more demands on the parameters of ignition coils, as well as their strength and durability [1]. Hidden defects, technical and reliability problems affect the quality and lifetime of ignition coils [2, 3]. Another problem is the low effectiveness and usefulness of engineering tools (analytical methods, approximate formulas) due to the complexity of the problem and the scale of the system [4, 5]. Implementation of some numerical, approximated methods, assuming some assumptions and simplification of the constructed models are justified due to:

1. occurring field phenomena in the system of turns (large number of turns, defects in arrangement, skin effect, displacement, proximity phenomena all dependent on frequency);
2. no possibility to analyze single coils;
3. the fact that pulse waveforms require time analysis and the worst-case consideration (signal band up to kHz);
4. the possibility of multi-variant analysis in order to reduce the costs of production preparation, estimating the efficiency of systems and reliability.

Case description

Strict parameters, such as discharge current or secondary voltage, are often selected by manufacturers at the limit of the strength of the materials used. An example is a set of coils: primary and secondary. The turn ratio is on the order of 1:100, and the secondary winding requires the proper arrangement of a huge number of turns. The guarantee of reliable operation is the proper division of the winding into sections or its proper winding on the bobbin. It is technologically difficult to implement. There are situations in which, when winding a coil, an undesirable change in the location of a given coil occurs. This creates a risk of an electric discharge between such turns. This may result in lowering of the induced secondary parameters or even shortening the lifetime of the ignition coil.

The construction of the ignition coil (Fig. 1) consists of primary [A] and secondary windings [B], which are wound on the bobbins and a core made of a package of magnetic steel laminations [C, D]. The whole is potted with epoxy resin [E], in a plastic housing [F], with a low voltage connector with terminals [G] and a high-voltage outlet for connecting the ignition cables or through a rubber sleeve [H] directly with the spark plug. An additional element used to determine the proper operating point [6] is a permanent magnet [I], the properties of which are the subject of the research described in this article.

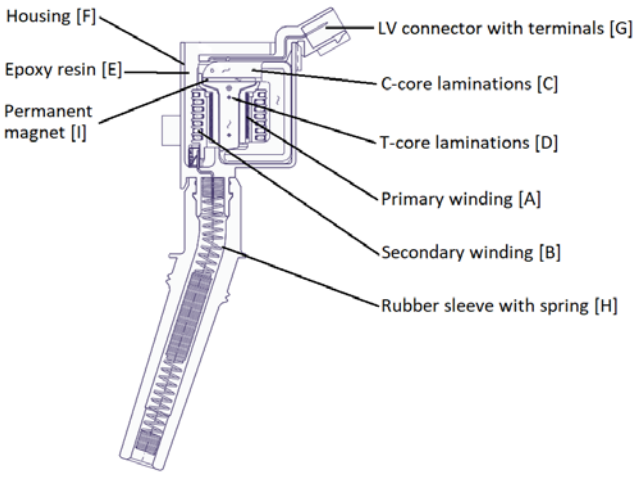

Fig. 1. Cut through view of analyzed ignition coil

Analytical model

The parameters characterizing the coils from the primary side are its resistance, inductance, supply voltage and current flowing through the winding. The power supply is usually realized by connecting the voltage from the battery, therefore the value of 14 V was adopted for the analysis. The peak value of the current in the primary coil depends on the time of energizing the winding. These values are in the order of 6 – 15 A depending on the demand. The secondary side can be described by winding resistance R_2, inductance L_2, output voltage, discharge current, discharge duration and spark energy [7]. High

voltages can be as high as 45 kV, but the standard level is 30 kV. The discharge current and its duration translate into the spark energy calculated on their basis.

The time-varying voltage on the secondary side is given by the formulas (1-2)

$$(1)\quad u_{c2j} = L_{2j}\frac{di_2}{dt} - M_{1,j}\frac{di_1}{dt} + \sum_{\substack{i=1\\ i\neq j}}^{N} M_{2i,j}\frac{di_2}{dt} + R_{2j}i_2$$

$$(2)\quad \sum_{j=1}^{N}\left(L_{2j}\frac{di_2}{dt} - M_{1,j}\frac{di_1}{dt} + \sum_{\substack{i=1\\ i\neq j}}^{N} M_{2i,j}\frac{di_2}{dt} + R_{2j}i_2 \right) + u_{\sup} + u_{Rp} = 0$$

where: N – number of sections in the secondary coil (j = 1,…,N), u_{c2j} – secondary coil voltage on j-section, L_{2j} – secondary coil inductance of j-section, R_{2j}– secondary coil resistance of j-section, i_1 – primary coil current, i_2 – secondary coil current, $M_{1,j}$ – primary coil magnetic coupling, $M_{2i,j}$ – secondary coil magnetic coupling, u_{sup} – suppressor resistor voltage, u_{Rp} – spark plug resistor voltage.

Using matrix notation, the generalized inductance of the secondary winding is expressed by the matrix, formulas (3) – (5)

$$(3)\quad \mathbf{L}_2 = \begin{bmatrix} L_{21} & \cdots & M_{1,N} \\ \vdots & \ddots & \vdots \\ M_{N,1} & \cdots & L_{2N} \end{bmatrix}$$

$$(4)\quad \dim \mathbf{L}_2 = N \times N$$

$$(5)\quad i, j = 1,2,...,N$$

where: $\mathbf{L}_2$ – secondary coil inductance matrix,

A simplified ignition coil system [8] with the division of the secondary winding into a specific number of sections is presented in Fig. 2. Such a division allows for a more accurate analysis of the occurring phenomena and measurements of the voltage and current values in individual sections. As a load at the output of the secondary winding, an equivalent spark plug scheme is connected.

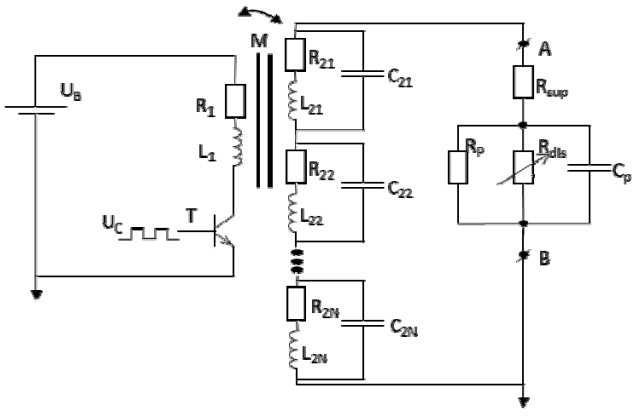

Fig. 2. Diagram of the ignition system with the division of the secondary coil into sections, where: U_B – battery voltage, R_1– primary coil resistance, L_1 – primary coil inductance, T – transistor, U_c – control signal, L_{2N} – secondary coil inductance of N-th section, R_{2N} – secondary coil resistance of N-th section, C_{2N} - secondary coil capacity of N-th section, R_{sup} – resistance of RFI suppressor inside spark plug, R_p – resistance of spark plug, R_{dis} – time variable, nonlinear resistance of discharge, C_p – capacity of spark plug.

The construction of the considered coil is intended to reduce the capacitance of the secondary winding. For this purpose, the secondary coil was divided into 7 sections (Fig. 3), separated by a layer of insulation (bobbin walls). Since the sections are connected in series, the resultant capacitance of winding becomes lower and related parasitic effects can be reduced. In order to decrease the capacitance, the dimensions of the winding layer (in the plane of the coil) are smaller than the height of the section and the overall dimensions of the section. Due to the macroscopic model of the secondary coil (arrangement of 7 sections, each section modelled as a uniform domain) and implementation of an approximate method of analyzing field phenomena (finite element method), capacitances between segments are inherently represented in the model. Capacitances between turns cannot be included due to restrictions of the applied numerical method (limited complexity of the FE model, limited number of degrees of freedom).

Analysis results

A parametric analysis of the described ignition coil system with a permanent magnet in the magnetic circuit was carried out. For this purpose, a field-circuit model was created in the Comsol Multiphysics program. Figure 3 shows the analyzed model with a mesh view for calculations. In areas where there may be a concentration of the magnetic field strength, the FE mesh is created using h-adaptation techniques.

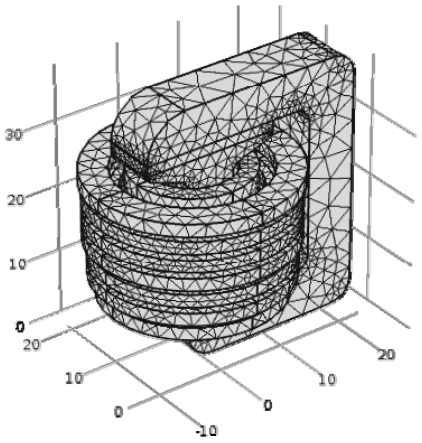

Fig.3. Mesh view of analyzed model

For the calculations, a constant number of turns of both windings, a constant cross-section of the winding wires and the material of the cores were assumed. The tested variable was the remanence value of the permanent magnet. The following B_r values were set for the simulation: 0.22 T, 0.44 T and 0.88 T. Input signals such as supply voltage, primary winding activation time and load also remained constant.

Figure 4 shows the time courses of charging the current in the primary winding. The influence of the remanence change on the shape of the characteristic is noticeable. With a higher magnetization value, the nonlinearity increases by the value of energy.

The voltage waveforms on the secondary side (shown in Figure 5) also show a change. As the remanence of the permanent magnet increases, the peak value of the first half-wave of high voltage and each subsequent one increases. Value of secondary voltage first peak (negative half-wave) is respectively 27.56 kV with B_r=0.22 T, 28.25 kV with B_r=0.44 T and 30.82 kV with B_r=0.88 T. That can be

read as an advantage. Negative effect is that there is also increasing value of second peak (positive half-wave). Value of secondary voltage second peak is respectively 7,25 kV with B_r=0.22 T, 9.29 kV with B_r=0.44 T and 15.30 kV with B_r=0.88 T.

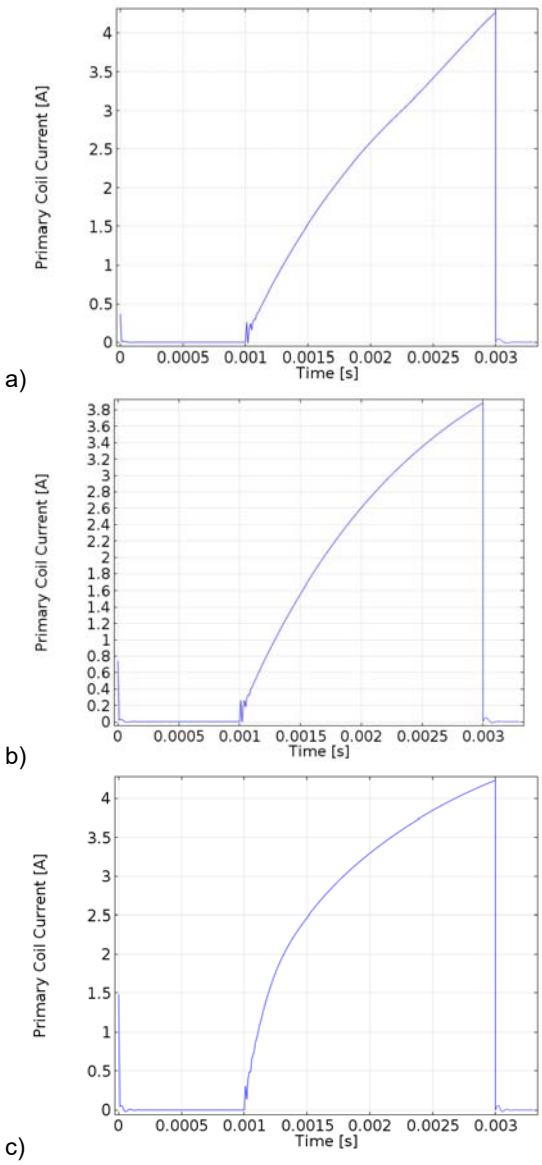

Fig.4. Primary coil current characteristics with permanent magnet remanence: a) 0.22 T, b) 0.44 T, c) 0.88 T

As a result of the field analysis, it was possible to observe the distribution of the magnetic field in the cross-section of the core and the permanent magnet. Figure 6 shows the value of magnetic induction at the time of commutation.

With a magnet remanence of 0.22 T, it can be seen that the vast majority of the core is in the saturation state. Increasing the remanence value is a noticeable decrease in magnetic induction.

Shifting the bias point of the magnetic core due to the introduction of permanent magnet leads to a change in the nature of the signals registered in the system. The maximum value of magnetic flux (Fig. 6) occurring at the end of the stage of energy accumulation (t <= 3 ms), according to increasing the remanence of the applied magnets. In this case, most of the magnetoguide does not enter into saturation state (compared to the system with lower magnet remanence). The main part of changes of magnetic flux takes place on the quasi-linear part of the B-H curve (out of the saturation range). This is reflected in the voltage waveform recorded on the secondary coil (Fig. 5). The maximum voltage on the secondary side increases above 30 kV.

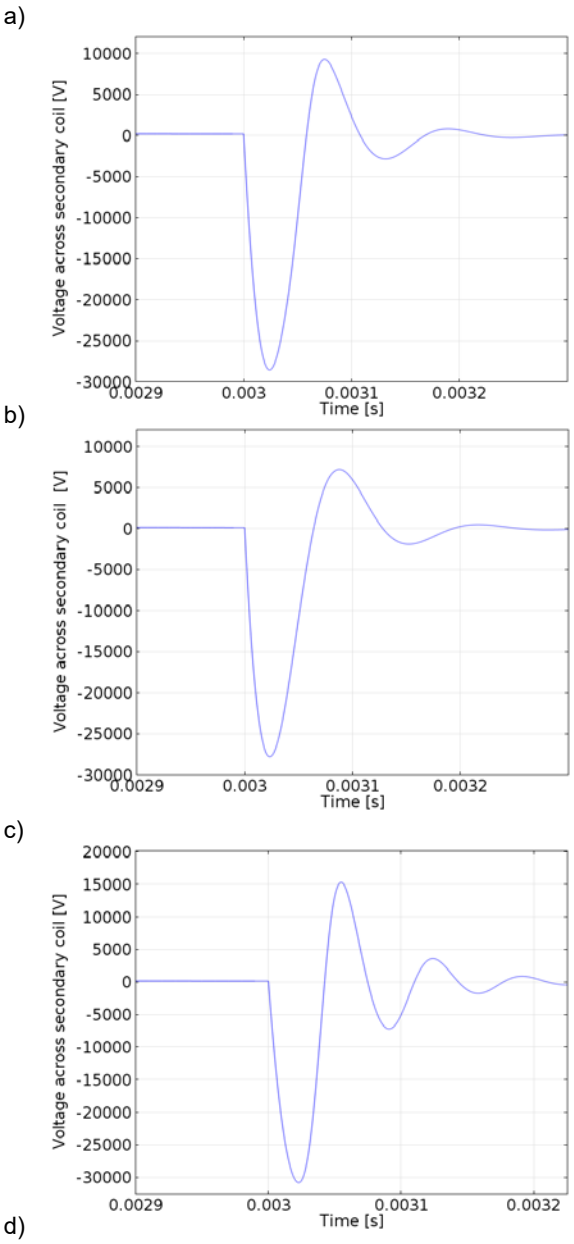

Fig.5. Waveforms of voltage on the secondary coil (primary circuit is open when t = 3 ms) for models with different permanent magnet remanence: a) 0.22 T, b) 0.44 T, c) 0.88 T

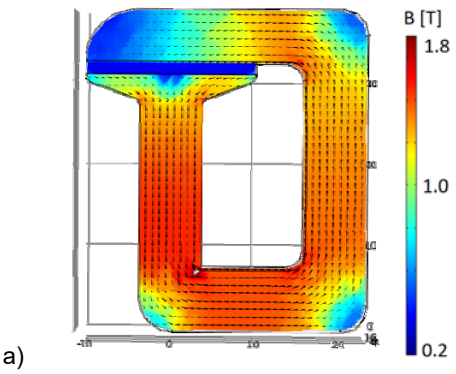

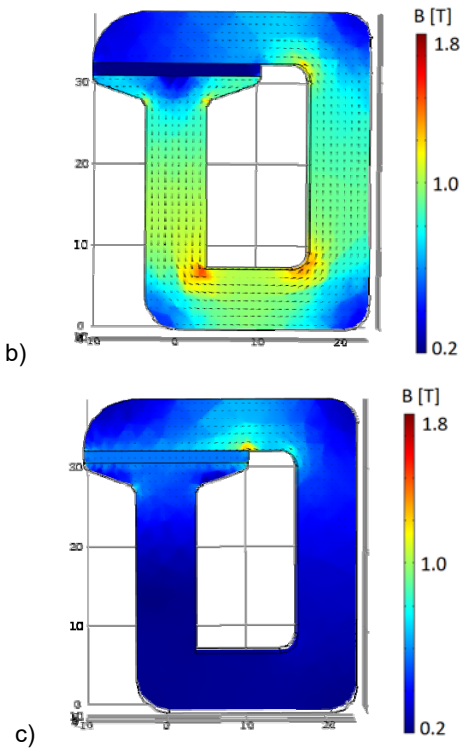

Fig.6. Magnetic induction on the cross-section of the core with permanent magnet remanence: a) 0.22 T, b) 0.44 T, c) 0.88 T

The waveforms of current in the primary winding (Fig. 4) also indicate that the value of energy transferred from the source to the ignition system increases. Due to the constant value of the supply voltage (U_B = 14 V = const), the current waveform in Fig. 4c indicates a higher energy efficiency of the system. In this way, additional possibilities were obtained to change the design of the system, adjust its properties to the requirements (e.g. lowering the supply voltage, changing the configuration of the secondary winding).

Conclusion

The integrated analysis of the field and circuit model allows the observation of phenomena when commutation (ignition) occurs in the system.

By modeling the arrangement of turns (winding segments), we can evaluate the coil structure, identify the measurement results and damages in the windings.

Based on time-domain calculations, field effects in critical regions of the magnetic core are available, as well as certain approximate currents and energies.

By selecting appropriate configurations of windings and the coil-core-permanent magnet system, we can obtain the required level of energy. The use of a stronger magnet in the system shifts the operating point and increases the energy on the primary and secondary side. Using magnet with remanence value two times greater we can get almost 3% higher secondary voltage and using four times greater we get even 10,5% higher secondary voltage. This also has negative effects, e.g. increase of high voltage oscillations to unacceptable levels. Second half-wave increases respectively for about 22% and 52,6%. All of this must be taken into account when selecting circuit parameters.

This work is supported by the Ministry of Education and Science Republic of Poland, under the industrial PhD program. This project is developed in SMP Poland Sp. z o.o. and Białystok University of Technology.

***Authors**: mgr. inż. Marcin Kalinowski, Politechnika Białostocka, Wydział Elektryczny, ul. Wiejska 45a, 15-351 Białystok, E-mail: marcin.kalinowski@sd.pb.edu.pl; dr hab. inż. Bogusław Butryło, prof. PB, Politechnika Białostocka, Wydział Elektryczny, ul. Wiejska 45a, 15-351 Białystok, E-mail: b.butrylo@pb.edu.pl;*

REFERENCES

[1] Kucera M., Sebok M., Kubis M., Korenciak D., Gutten M., Analysis of the Automotive Ignition System for Various Conditions, *Communications - Scientific Letters of the University of Zilina 2020, 22(4):144-152*

[2] Sebok M., Gutten M., Ostrica L., Kucera M., Makyda M., Analysis of distributorless ignition system, *Przegląd Elektrotechniczny* 2013, 89(7):25-28

[3] Stevenson R. C., Palma R., Yang C. S., Park S. K., Mi C., Comprehensive modeling of automotive ignition systems, *SAE* (Society of Automobile Engineers) *Technical Paper*, SP-2088, ISSN 0148-7191

[4] Zhu G., Pattabiraman K., Perini F., Rutland C., Modeling ignition and combustion in spark-ignition engines based on swept-volume method, *SAE Technical Paper*, SP-2018-01-0188, ISSN 0148-7191

[5] Zhang J., Dai S., Ma T., Xu, Y., Yan X., High-frequency impulse modeling and longitudinal insulation analysis of bifilar superconducting coil, *IEEE Transactions on Applied Superconductivity*, vol. 31, no 1, 2021.

[6] Chan H. L. , Cheng K.W.E., Cheung T. K., Cheung C. K., Study on Magnetic Materials Used in Power Transformer and Inductor, *IEEE Xplore, Conference: Power Electronics Systems and Applications, 2006. ICPESA '06. 2nd International Conference on,*

[7] Różowicz S., Voltage modelling in ignition coil using magnetic coupling of fractional order, *Archives of Electrical Engineering, 2019, VOL. 68(2), pp. 227–235*

[8] Różowicz S., Use of the mathematical model of the ignition system to analyze the spark discharge, including the destruction of spark plug electrodes, DE GRUYTER, *Open Phys. 2018; 16:57–62*